Journal of Optoelectronics and Advanced Materials Vol. 6, No. 1, March 2004, p. 23 - 38

REVIEW PAPER

TOWARD SUPER RADIATION TOLERANT SEMICONDUCTOR DETECTORS FOR FUTURE ELEMENTARY PARTICLE RESEARCH♣

G. Lindstroem[a*], E. Fretwurst[a], G. Kramberger[b,c], I. Pintilie[a,d]

[a]University of Hamburg, Institute for Experimental Physics, Luruper Chaussee 149, 22761 Hamburg, Germany
[b]Deutsches Elektronen Synchrotron DESY, Notkestraße 85, 22607 Hamburg, Germany
[c]Jozef Stefan Institute JSI, Jamova 39, 1000 Ljubljana, Slovenija
[d]National Institute of Materials Physics, NIMP, 77125 Bucuresti-Magurele, Romania

The principal of a semiconductor particle detector is briefly outlined and applications in several fields of fundamental and applied physics mentioned. Starting from the basic physics motivation in High Energy Physics (HEP) research, the further discussion then focuses on the use of these devices in present and future HEP experiments outlining especially the requirements for precise measurements of elementary particle tracks, a task ideally fulfilled by segmented silicon detectors. These developments have also initiated further applications in different fields as e.g. material analysis, medical imaging and space missions. In future HEP-experiments such devices will however face an unprecedented challenge imposed by extremely intense radiation fields. Basics of hadron and lepton induced radiation damage in silicon are described together with their implications on the detector quality. The following part of the report is then dealing with several approaches to improve the radiation tolerance of silicon detectors. Defect engineering of the semiconductor material, modified detector geometries and specific operational conditions are outlined. First results toward a complete understanding of detector degradation as caused by point and cluster defects are given and these promising successes may finally pave the way for developments of superior devices.

(Received August 28, 2003; accepted after revision February 9, 2004)

Keywords: High energy physics instrumentation, Elementary particle detectors, High resistivity FZ and epitaxial silicon, Radiation damage, Radiation induced defects, Defect engineering

1. Introduction

A semiconductor particle detector may be best envisioned as an ionization chamber in which the conventional sensor gas is replaced by a high purity solid state media. The first developments reach back to 1949 [1] and had been soon recognized to be superior as compared to conventional gas ionization chambers since the solid state material allowed for compact radiation detectors. Developments had focused on both silicon- (for ionizing particle detection) and germanium detectors (for gamma ray spectroscopy). Both semiconductors had been widely studied as the basic material for electronic devices and hence detector developments could build on an invaluable base of industrial knowledge.

This report is focusing on silicon particle detectors only. The basic structure is an asymmetric junction diode (p^+nn^+) where the p^+ and n^+ electrodes are normally produced by ion implantation and the bulk material is of extreme high purity with a very low donor doping concentration (Fig. 1). The thickness of the low doped bulk ranges from a few hundred microns up to millimeters and the applied reverse bias voltage (depletion voltage) needed to extend the electric field throughout this thickness is in the or-

♣ work performed in the frame of the CERN-RD50 collaboration
* Corresponding author: gunnar.lindstroem@desy.de

der of 10^2 to 10^3 Volt. Present day silicon detectors exhibit superior properties, so far unsurpassed by any other sensor material:

- excellent energy resolution, governed by a low ionization energy, a small Fano factor and complete charge collection due to negligible trapping
- fast signal response, as resulting from large electron and hole mobility and large allowable electric field strengths
- large signal to noise ratio and small dissipation power as the wide band gap and high material purity leads to small dark currents

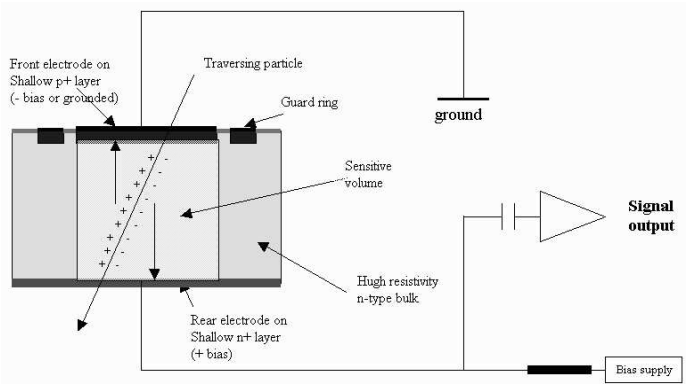

Fig. 1. Simplified principle of a silicon particle detector.

In addition these detectors are very compact, can be operated in ambient atmospheres, at room temperature and at moderate voltages. Detectors manufactured on high resistivity silicon (10-30 kΩcm) allow a depletion thickness of up to millimeters, sufficient enough to stop energetic charged particles and thus precisely measure their total energy in nuclear physics experiments or also for soft X-ray spectroscopy in material investigations. Employment of the planar process for detector processing had then led to the development of segmented devices (microstrip- and pixel-detectors) enabling precision measurements for traversing ionizing particle tracks as necessary for high energy physics [2]. Finally the possible integration of sensor and electronics on one single chip is an additional benefit, presently exploited for several applications. Numerous applications also outside the high energy physics experiments are nowadays employing multi-electrode configurations allowing superior position and energy detection, as e.g. in different types of drift detectors and several variances of charged coupled devices. Pixel detectors are also widely used as imaging devices for soft X-ray detection as diagnostic tools in e.g. medicine. Surveys of state of the art developments may be found in text books and topical conferences, see e.g. [3-11].

2. Segmented silicon detectors, indispensable tools for elementary particle physics

The interplay between experiments and theoretical descriptions in elementary particle research has led to an ever deepening understanding of fundamental physics where each further step had led to a much better understanding. The “standard model” can already well describe the world around the building blocks of matter (quarks, leptons). It combines three of the four fundamental forces, the electromagnetic, the weak and the strong one. The interactions are carried by exchange particles (gamma quant for the electromagnetic, W-and Z-boson for the weak and gluons for the strong force). The gravitational force (being small enough to be neglected in the micro cosmos) is not yet included in this description but may well be within the next but not yet experimentally proven “supersymmetric” extension of the standard model. Still another open topic involves the question of the origin of the particular mass values for the building blocks of matter. Physicists believe that the Higgs-field may be responsible for this and they are therefore, looking ahead to find the particle to be associated with this field, the Higgs-boson. Along

the lines of the sketched theoretical ideas the energy needed for experimental proof had successively to be enlarged. In fact extremely high energies are needed and these are reached today in colliding beam experiments where hadron beams (e.g. proton as in the forth-coming CERN Large Hadron Collider LHC) or leptons (electrons and positrons as in the planned TeV energy linear collider TESLA) are interacting with each other de-livering the required centre of mass energies (14 TeV for LHC, 500-800 GeV for TESLA), [12,13].

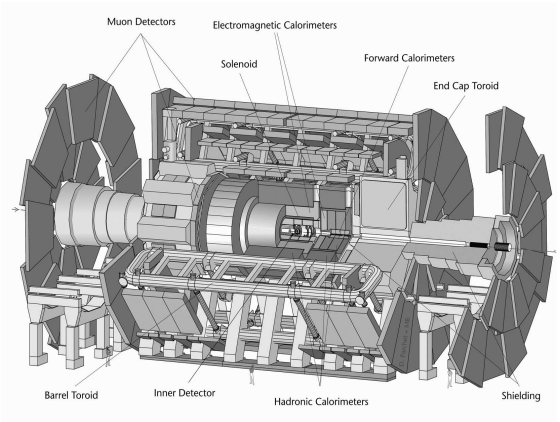

Fig. 2. The ATLAS detector for LHC, CERN, Characteristics: width 44 m, diameter 22 m, weight 7000t [14].

A typical LHC-experiment (ATLAS) is depicted in Fig. 2 [14]. The very large and complex setup consists mainly of an "inner detector" responsible for precise measurements of the primary particle tracks emerging from the interaction, surrounding calorimeters in which the total energy of primary particles can be measured and outer layers of sensors responsible for the detection of muons traversing the other components with much less interaction. Each bunch crossing will lead to about 30 collision events and the emerging particles or particle jets have to be measured with high position precision of about 10 μm. Successive beam bunches are colliding every 25 nsec and thus the particles have to be tracked with a time resolution of about 10 nsec in order to ensure that they originate from the same event.

These extreme requirements for spatial and time resolution can best be fulfilled by segmented silicon detectors either as pixel- or as microstrip devices (Fig. 3) favored also by their ready availability and comparatively low cost. The ionization of a minimum ionizing particle (mip) in a 300 μm thick detector leads to a signal of 25×10^3 electron charges and current low noise amplifier electronics guarantee a necessary signal to noise ratio of $S/N \geq 15$. Many cylindrical layers and forward wheels are needed to ensure the required track precision employing e.g. 200 m² of silicon detectors for the CMS detector at LHC [16].

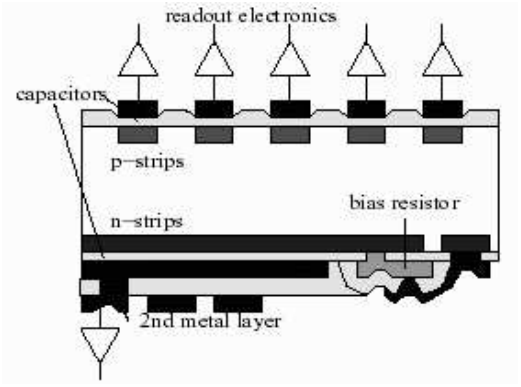

Fig. 3. Principle of a doublesided strip detector as to be used in the CMS experiment at LHC [15].

3. Radiation damage, the challenge in future high energy physics experiments

Silicon detectors, used primarily in the inner detector region of the forthcoming HEP experiments face an extremely hostile radiation field, mainly of hadronic particles. The reason for this is that the interesting events, which could e.g. lead to the discovery of the Higgs-boson, are expected to be extremely rare. Therefore, the collision intensity of the beam bunches, measured as "luminosity" has to be as large as possible. For LHC the luminosity is foreseen to be $L = 10^{34}$ cm^{-2}s^{-1}, the center of mass energy 14 TeV and the interaction rate is 1×10^9 proton-proton collisions per second. Close to the interaction region the primary produced pions are the dominant component, causing a 1 MeV neutron equivalent fluence of 3×10^{15} cm^{-2} (see section 4) for the innermost pixel layer during the foreseen 10 years operational period. The radial dependence of the total particle fluence is given in Fig. 4. Note that in contrast to the high energetic primary pions the neutron spectrum is centered in the MeV-range as it originates from secondary reactions in the calorimeter bulk, scattered back into the inner detector ("albedo neutrons").

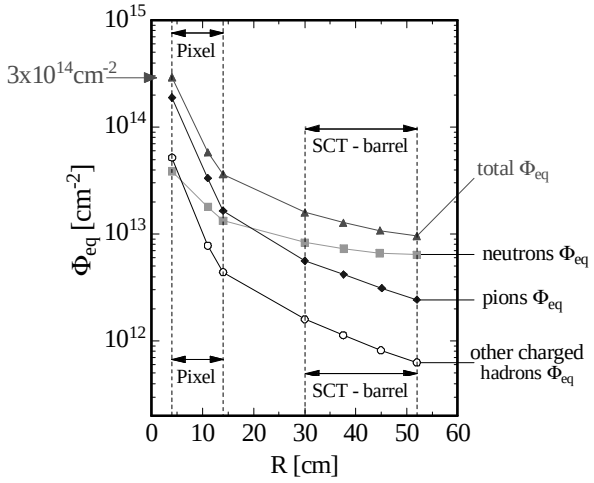

Fig. 4. Hadron fluences per each year expected in the ATLAS inner detector at LHC [19].

An even much larger challenge will be imposed by the planned upgrade of the LHC (SLHC), to be envisioned for the time after 2012, with a 10 times higher luminosity leading to an equivalent fluence of 1.6×10^{16} cm^{-2} for the innermost pixel layer during a 5 years operational period. In this case no viable solution exists so far for any detector technology which would have the required radiation tolerance [17].

4. Non ionizing energy loss NIEL

The bulk damage in silicon detectors caused by hadrons or higher energetic leptons respectively gammas is primarily due to displacing a Primary Knock on Atom PKA out of its lattice site. The threshold energy for this process is ~ 25 eV. Such single displacements resulting in a pair of a silicon interstitial and a vacancy (Frenkel pair) can be generated by e.g. neutrons or electrons with an energy above 175 eV and 260 keV respectively. Low energy recoils above these threshold energies will usually create point defects. However, for recoil energies above about 5 keV a dense agglomeration of defects is formed at the end of the primary PKA track. Such disordered regions are referred to as defect clusters. The kinematic lower limits for the production of clusters are ~35 keV for neutrons and ~8 MeV for electrons. In addition to the hard core nuclear interaction being dominant for neutrons proton reactions are also subjected to Coulomb interactions leading to low energy recoils below the cluster threshold. Thus, we would expect a mixture of homogeneously distributed point defects and clusters in this case. This distinct difference between neutron and proton induced damage effects is depicted in Fig. 5.

It should be noted here that the radiation damage caused by Co-60 gammas is primarily due to the interaction of Compton electrons having a maximum energy of only 1 MeV. Hence in this case cluster production is not possible and the damage is exclusively due to point defects.

Experimental findings have led to the assumption that damage effects produced in the silicon bulk by energetic particles may be described as being proportional to the so-called displacement damage cross section D. This quantity is equivalent to the Non Ionizing Energy Loss (NIEL) and hence the proportionality between the NIEL-value and the resulting damage effects is referred to as the NIEL-scaling hypothesis. On the basis of the NIEL scaling the damage efficiency of any particle spectrum can then be calculated as that of an equivalent 1 MeV neutron fluence.

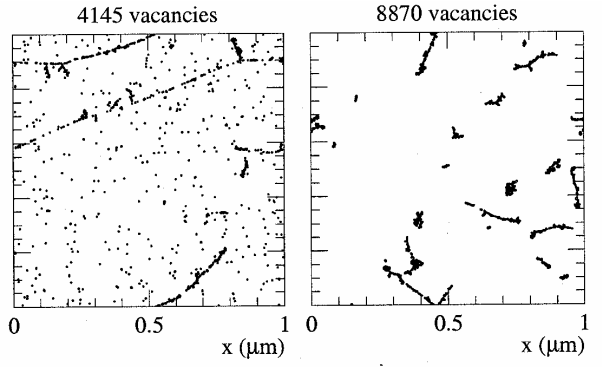

Fig. 5. Distribution of vacancies produced by 24GeV/c protons (left) and 1 MeV neutrons (right) [18].

In Fig. 6 the normalized NIEL values are plotted as function of energy (for details see [19]). NIEL scaling and its limitations is extensively discussed in [18]. Regardless of possible deviations in certain cases, the NIEL scaling should always be applied as a first approximation of the damage efficiency. Any damage results are therefore plotted as function of the 1 MeV neutron equivalent fluence. Irradiations by a Co-60 gamma source will also lead to radiation damage in the silicon bulk. In this case usually the irradiation intensity is measured by the dose-value. However, this is not an adequate quantity as it refers only to ionization effects and not to the displacement damage. Using the details of the Co-60 decay, the finally produced electron spectrum in silicon and its proper NIEL folding one gets a NIEL value of 4.7×10^{-3} MeVmb, extremely small compared to 1 MeV neutrons (95 MeVmb). With this, e.g. a 100 Mrad Co-60 gamma dose corresponds to a hadron fluence of $\Phi_{eq} = 9.3 \times 10^{12}$ cm^{-2}.

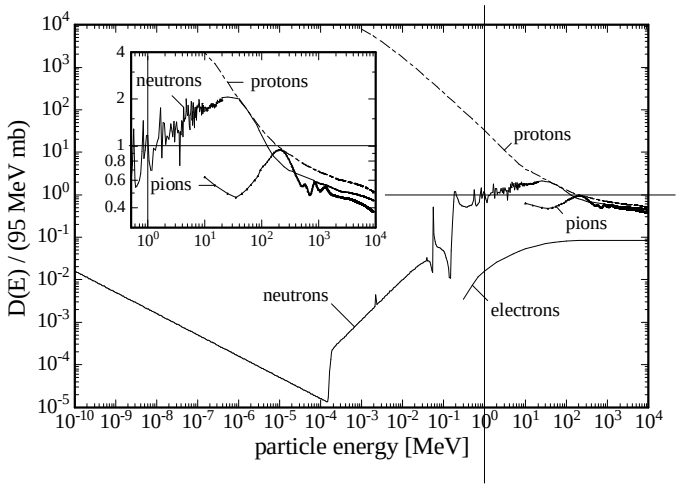

Fig. 6. Non Ionising Energy Loss NIEL for different particles [19].

It should be emphasized again that the NIEL scaling can only be regarded to be a rough normalization as it disregards the specific effects resulting from the energy distribution of the respective Si-recoils. While e.g. the irradiation by MeV-neutrons leads to a recoil spectrum with a high average energy, resulting in predominant cluster formation, charged particle interaction are also subject to Coulomb interaction with a pronounced low energy tail in the recoil spectrum. These low energy recoils would then more likely cause isolated point defects (see Fig. 5).

5. Survey of damage induced deterioration in detector performance

Three main deterioration effects are seen in high resistivity silicon diodes following energetic hadron irradiation, these are:

- Fluence proportional increase of the reverse current, influencing accordingly the dissipation power and electronic noise level.
- Change of the doping concentration with severe consequences for the operating voltage needed for total depletion.
- Increase of charge carrier trapping deteriorating the charge collection efficiency and thus together with the noise increase reducing the signal to noise ratio.

The implications of severe radiation damage to be expected in the LHC experiments had initiated the formation of an international collaboration RD48 (ROSE collaboration) at CERN, focusing entirely on the systematic study of these effects and also trying to improve the radiation hardness of state of the art silicon detectors. Much of the discussion presented here is due to the combined work of that collaboration [20-22]. For the even much larger challenge implied by the planned upgrade of the LHC (SLHC) a new collaboration was formed in 2002, the CERN RD50 collaboration. In addition to an even more improved radiation tolerance of silicon detectors it aims also at investigating several alternatives [23- 26]. In the following only the main features of damage effects are summarized, which are apparent in standard (non radiation hardened) silicon detectors.

5.1 Reverse current

The damage induced increase of the reverse current exhibits a simple dependence on particle fluence and temperature. When surface contributions can be disregarded (this is normally the case), it is entirely due to the generation of electron/hole pairs in the silicon bulk. The increase of the reverse current ΔI is in this case proportional to the volume of the detector bulk and to the equivalent irradiation fluence Φ_{eq} thus demonstrating an excellent proof for the validity of the NIEL hypothesis (Fig. 7). Its temperature dependence follows a simple Boltzmann function with the gap energy (1.1 eV in silicon) as leading parameter. In order to overcome the resulting deterioration effects in the detector performance a moderate cooling is hence sufficient. At LHC the operating temperature will be kept at -10^{o}C power and noise level even for thus ensuring a sufficiently low dissipation the largest fluence values close to the beam interaction.

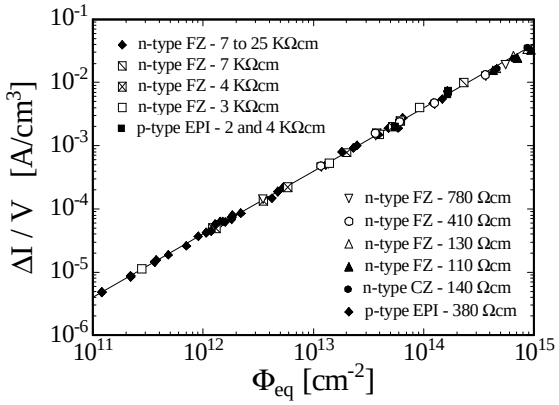

Fig. 7. Damage induced bulk current as function of 1MeV neutron equivalent particle fluence [28].

Fig. 7 demonstrates also that the factor α in $\Delta I/V = \alpha\Phi$, often called the current related damage rate, does not depend on the conduction type and resistivity of the silicon, used for the detectors [28].

5.2 Depletion voltage

The depletion voltage V_{dep} necessary to fully extend the electric field throughout the depth d of an asymmetric junction diode is proportional to the effective doping concentration N_{eff} and d^2. The equation holds not only for the original n-type silicon with N_{eff} governed by an abundance of donors but also after severe irradiation when the material in the depleted region had undergone a space charge sign inversion thus leading to an equivalent p-type behavior. The dramatic effect of hadron irradiation on the effective doping concentration and hence depletion voltage is shown in Fig. 8 (see [29]). The increase of the needed depletion voltage after "type inversion" is beyond any tolerable value and this effect had then been the major impact for the radiation hardening efforts.

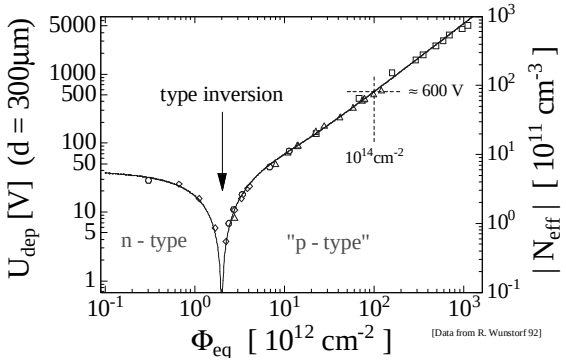

Fig. 8. Effective doping concentration in standard silicon, measured immediately after neutron irradiation [29].

5.3 Charge collection efficiency

Due to the generation of deep electron or hole traps the charge generated by a traversing particle may be partly trapped along its path to the respective electrode and such not able to contribute anymore to the observed signal height. Measurements for either electron or hole trapping can be performed by illuminating the diodes from the p^+ respectively n^+ electrode by ultra-fast IR-laser pulses with an appropriate wavelength to assure shallow absorption. A time resolved analysis of these pulses will then reveal the effective trapping times τ_{eff}. As expected the trapping probability $1/\tau_{eff}$ is increasing linearly with the irradiation fluence (Fig. 9, [30]).

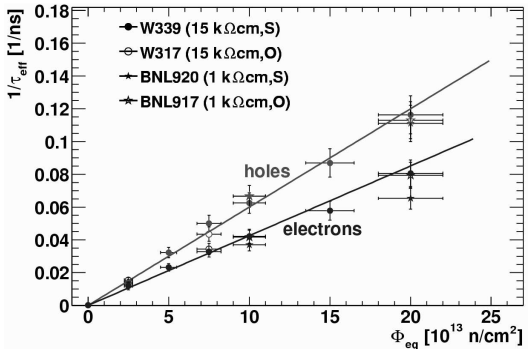

Fig. 9. Trapping probability $1/\tau_{eff}$ measured for electrons and holes in standard (S) and oxygen enriched silicon (O) [30].

5.4 Annealing studies

As the detectors at LHC and other experiments will have to operate at extended periods of years it is important to know how the performance will develop after the initial damage due to annealing effects. As it is impossible to check the development of damage effects for such long durations the underlying kinetic effects were accelerated by keeping the detectors after irradiation at elevated temperatures and extract the temperature dependence of all relevant parameters. This way the needed compression of a 10 years subsequent damage investigation to lab experiments of only weeks was made possible.

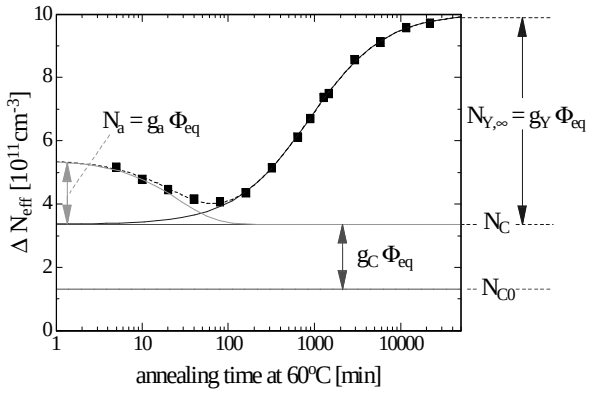

Fig. 10. Change of the measured space charge concentration as function of annealing time at T = 60 °C [28].

Fortunately, it turns out that the current related damage rate α is monotonically decreasing with time, which is reassuring for the detector performance. Even after long storage the current will always be lower than the value obtained after the initial damage. Also only a very moderate increase of the trapping probability and hence decrease of the charge collection efficiency was observed. In contrast the annealing implications for the effective doping concentration are severe (Fig. 10) and are even of more concern than the initial change as shown in Fig. 8. Plotting the change of the effective doping concentration $\Delta N_{eff} = N_{eff,0} - N_{eff}(\Phi_{eq})$ as function of annealing time for a given annealing temperature one may decompose the overall behavior into a short term "beneficial" part (decrease of the initial change) with amplitude N_A, a time independent "stable" component N_C and a "reverse annealing" part with a saturation value N_Y. For "standard" silicon all three components are proportional to the hadron fluence. A systematic investigation of the temperature dependence of the given parameters allows a projection on the real LHC operational scenario.

6. Radiation hardening, the RD48-approach

The key idea of the CERN-RD48 strategy implied that the radiation tolerance of silicon can be improved by adequate defect engineering [20-22]. Defect engineering involves the deliberate addition of impurities in order to reduce the radiation induced formation of electrically active defects or to manipulate the defect kinetics in such a way that less harmful defects are finally created. RD48 relied on carbon and oxygen as the key ingredients for reaching this goal. A wide range of oxygen and carbon concentrations had been investigated using different process technologies. It was finally found that oxygen plays a significant role for improvements of the radiation tolerance while carbon has an adverse effect. The necessary oxygen enrichment can easily be achieved by a post-oxidation diffusion of oxygen into the silicon bulk. This so-called DOFZ process (Diffusion Oxygenated Float Zone) had been performed at temperatures between 1100 and 1200 °C and with durations between several hours up to 10 days. The DOFZ process technology was meanwhile successfully transferred to several detector manufacturing companies and is e.g. employed in the production of pixel detectors for both LHC-experiments ATLAS and CMS [15, 27]. RD48 results presented here, are taken from [19-22] and proper citations are given there.

6.1 Results for hadron irradiation

As the change of the effective doping concentration N_{eff} with fluence as well as its annealing behavior is rather complex (see above), it was found useful to perform rapid comparisons of the radiation hardness of detectors processed on different material almost online during the irradiation experiments. However, larger fluences imply also longer irradiations and normally simultaneous damage and annealing cannot be avoided. In order to overcome these problems a special recipe had been devised giving results, which are rather independent on the irradiation history. Making use of the fact that the annealing of the damage-induced change of N_{eff} follows a rather flat dependence around 10 days storage at room temperature, corresponding to about 4 minutes at 80 °C (equivalent to 80 minutes at 60 °C, see Fig. 10), a so-called CERN-scenario measurement was used. After each successive irradiation step the device under test is stored for 4 minutes at 80 °C and then the normal C/V technique is applied for measuring the depletion voltage.

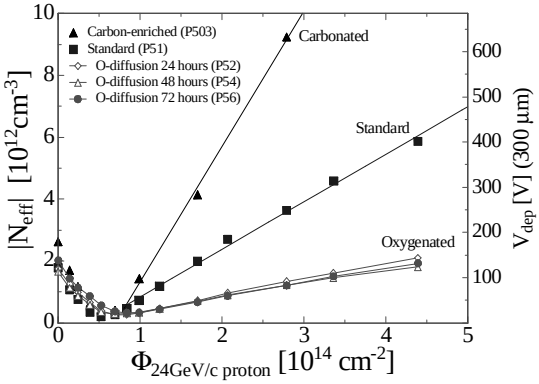

Fig. 11. Influence of carbon and oxygen enrichment on the change of N_{eff} as function of fluence (see text). Multiply the fluence values by 0.62 for getting Φ_{eq}. [31].

Fig. 11 shows a comparison between standard, carbon- and oxygen enriched silicon as irradiated by 24 GeV/c protons at the CERN PS irradiation facility. The minimum in these curves for $|N_{eff}|$ is displaying the fluence for which the material becomes type inverted, and the increase at higher fluence values is almost linear. The slope of this branch is a very good measure of the radiation tolerance. It is clearly seen that oxygen enrichment reduces the slope considerably by about 1/3 of that for standard silicon while carbon-enrichment proves to have an adverse effect. However, although pion and proton irradiation exhibit the same improvement of DOFZ material, neutron damage does not result in a similar reduction.

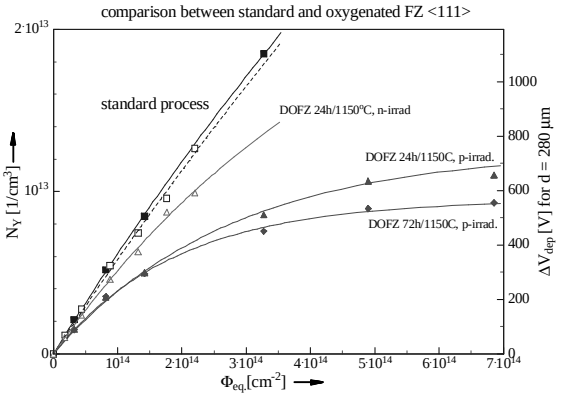

Fig. 12. Reverse annealing amplitude after neutron (open symbols) and proton irradiation (filled symbols) [19].

As already mentioned, this CERN-scenario technique allows only the measurement on one relevant damage parameter, namely the change of N_{eff} around the minimum of the annealing function. A different but much more time consuming approach, uses a set of detectors which are irradiated individually with different fluences and thereafter subjected to full annealing cycles at an elevated temperature for accelerating the annealing kinetics (see section 5.4). A detailed discussion of such annealing experiments can be found in [28]. Here we will present the general behavior regarding the DOFZ benefits seen for the reverse annealing amplitude N_Y. Standard silicon exhibits an almost linear dependence of N_Y with fluence while DOFZ silicon shows strong saturation at large fluences (Fig. 12). The difference between 24 and 72 h oxygen diffusion is not very large. However, it is interesting that, contrary to previous investigations, also some improvement after neutron irradiation is seen. This saturation effect as well as an observed increase of the reverse annealing time constant for DOFZ silicon offer an additional safety margin for detectors at room temperature every year during maintenance periods but otherwise cooled during the entire 10 years operation (defect kinetics frozen). With all damage parameters relevant for N_{eff} its change can then be calculated for pronged operation in any given hadron radiation environment. Such projections for LHC are shown in Fig. 13. It is obvious that only the DOFZ method guarantees the required operational lifetime, as bias voltages are technologically limited to less than 1000 Volt.

The beneficial effect of oxygenation in low phosphorus doped silicon was nicely predicted by the defect kinetics model of MacEvoy [33]. Another model [34] has suggested that for highly phosphorus doped silicon an oxygen enrichment will rather degrade than improve the radiation hardness of the material. However the latter model refers to a case which is not applicable for LHC experiments since the depletion voltage for such highly doped Si ([P] = 10^{14} cm^{-3}) would be about a factor 100 higher as needed for devices manufactured on standard high resistivity float zone silicon.

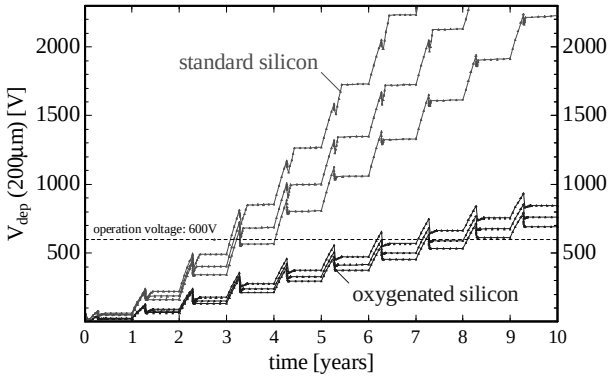

Fig. 13. Damage projections for the ATLAS pixel detector (r = 4 cm), yearly warm up: 14, 30 and 60 days [22].

According to systematic investigations of the damage induced increase of the bulk generation current as well as the increase of the charge carrier trapping and the corresponding degradation of the charge collection efficiency no beneficial effect was found for DOFZ silicon. More details on these studies can be found in [28,30]. It should be emphasized that both effects follow strictly the NIEL scaling.

6.2 Correlations between defect formation and detector performance

Systematic studies for defect engineering are finally only possible if the correlation between defect formation and the detector performance would be known. Numerous investigations have been undertaken for characterization of damage induced defects and evaluation of their introduction rates in detector grade silicon, especially using DLTS (Deep Level Transient Spectroscopy) and TSC (Thermally Stimulated Current) techniques, showing a lot of relevant results (for references see [28]). A promising correlation has been reported between the cluster formation as visible in the double vacancy defect and the damage related current [32]. Other studies have given a lot of detailed information of defect kinetics visible in the changes during prolonged annealing or as function of temperature, an example of which is

shown in Fig. 14. However, despite many partially useful attempts it had been so far not possible to quantitatively fully understand the detector performance on the basis of such microscopic data. In the following an examples is given, which is regarded to be promising in this respect. It refers to the distinct difference between neutron and proton irradiation as seen e.g. in Fig. 12, strongly violating the NIEL scaling hypothesis outlined in section 4. Although this so-called proton-neutron puzzle is still not completely understood, the results displayed in Fig. 15 may give an insight. The double vacancy defect E4 is surely related to cluster formation while E2 is composed of the A-center (VO_i) and a carbon complex (C_iC_s), both being isolated point defects. Therefore, the ratio of the introduction rates g(E2)/g(E4) measures the point defect generation with respect to cluster formation. The results relate nicely to the simulation data of Fig. 5. Point defect formation plays a much larger role in damage caused by charged particles than by neutrons.

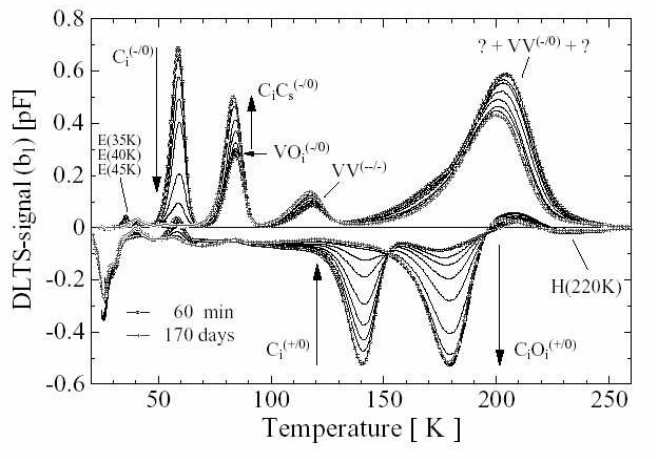

Fig. 14. Room temperature annealing effects as seen in DLTS spectra between 1 h and 170 days after irradiation [28].

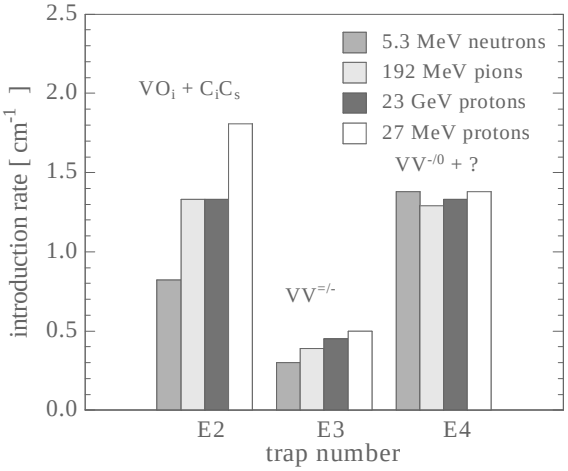

Fig. 15. Generation rates for E2 and E4 from neutron, pion and proton damage; g(E2)/g(E4) = 0.6 for neutrons, 1.3 for 27 MeV protons [19].

7. Understanding of the oxygen effect, an insight into defect engineering

Keeping in mind that the beneficial effect of oxygen enriched silicon with respect to the change of N_{eff} is predominantly observed in charged hadron damage and that the generation of point defects is

enhanced in such radiation fields one may assume that the oxygen effect should be maximal for ^{60}Co gamma irradiation, since low energy gamma damage results only in a creation of isolated point defects (see section 4). This had led to a detailed investigation of gamma induced damage both as to microscopic measurements by DLTS and TSC (Temperature Stimulated Current)-techniques as well correlations with deteriorations of the detector performance. Though already started within the RD48 collaboration most of the following results had been obtained in the frame of RD50.

The long suspected candidate that could explain the improvement obtained by oxygen enrichment is the acceptor like V_2O-center, a deep defect in the middle of the forbidden gap [33]. ^{60}Co γ-irradiation studies have shown that the improvement obtained with DOFZ silicon is in this case much more pronounced than observed after hadron irradiation [35]. Based on these early results the Hamburg group had then undertaken a thorough systematic study and the main results are outlined in the following. Fig. 16 demonstrates the development of the depletion voltage V_{dep} or effective space charge concentration N_{eff} with the accumulated dose, for standard float-zone (STFZ) and three differently oxygenated float-zone (DOFZ) devices manufactured from <111> silicon. The detectors manufactured from standard material show the well known effect of space charge sign inversion (SCSI). Initially the depletion voltage drops to a minimum value at a specific dose of about 200 Mrad (equivalent to a 1 MeV neutron fluence of 2×10^{13} cm^{-2}, see section 4), in good agreement with measurements for hadron damage (Fig. 11) before it increases again. In contrast to this behavior, for all oxygenated devices a small, monotonically and non-linear increase of the effective space charge density is observed. This implies that the space charge becomes more positive possibly caused by an introduction of donor like defects (see below). In contrast to hadron induced damage one observes also an improvement in the leakage current. DOFZ diodes exhibit a 3 times smaller current related damage rate than those manufactured from standard silicon. Related to the equivalent hadron fluence in both cases the damage rate is considerably lower (by at least a factor of 5 for standard silicon) than observed after hadron damage. This points again to the suspected fact that the current increase seen after hadron damage is much more dominated by cluster formation, completely absent in gamma damage.

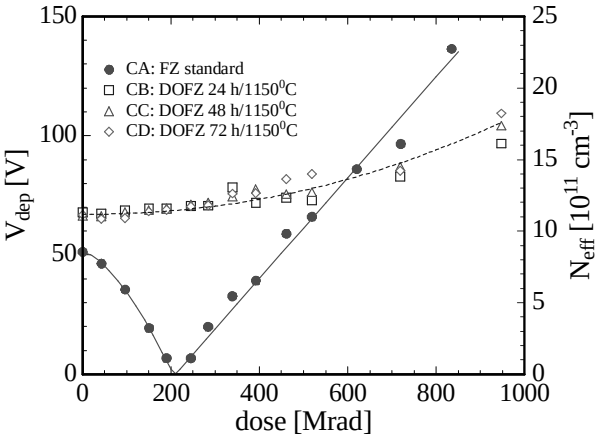

Fig. 16. Effective doping concentration as function of gamma dose for standard (filled) and DOFZ silicon (open symbols) [39].

These changes of the macroscopic detector properties had only recently been correlated with results of detailed microscopic studies [36-38]. Two close to midgap acceptor levels were discovered which are denoted as I- and Γ-defect (Fig. 17). The I center is most likely the V_2O defect while the Γ level cannot be attributed so far to a known defect. As expected for the V_2O center and also observed for the I-defect, both introduction rates are strongly reduced in oxygen rich material.

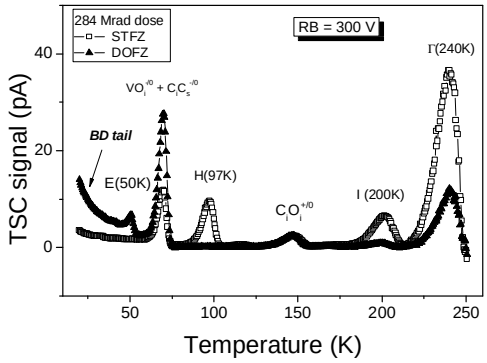

Fig. 17. TSC-spectra for standard (STFZ) and Oxygen enriched (DOFZ) diodes after Co-60 gamma irradiation with 285 Mrad [38].

The identification of the I-defect with V_2O, as proposed here, is further verified by the fact that the isochronal annealing shows an almost identical behavior as originally observed in EPR-studies [40]. A comparison is shown in Fig. 18.

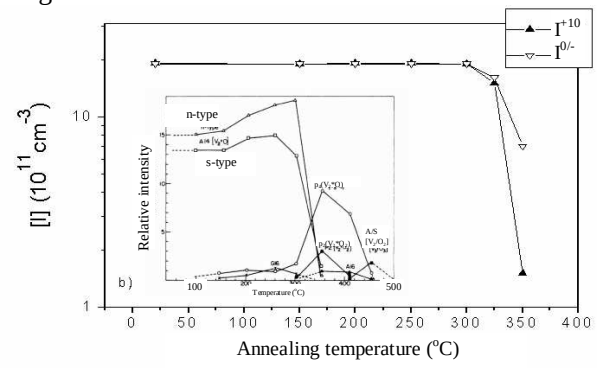

Fig. 18. Isochronal annealing of the I-defect after 400 Mrad Co-60 gamma irradiation [40], [41].

In oxygen doped sensors an introduction of shallow donors had been observed in TSC-spectra (BD in Fig. 17) very likely to be identified with a bi-stable thermal double donor TDD. Using the analyzed defect level parameters and the introduction rates as function of the gamma dose it was then shown that both the change in the effective doping concentration and the reverse current of standard and oxygenated silicon detectors can largely be attributed to the creation of these three defect centers, as demonstrated in Fig. 19. This result is an absolute first in the long search for an understanding of macroscopic damage effects by defect analysis [38].

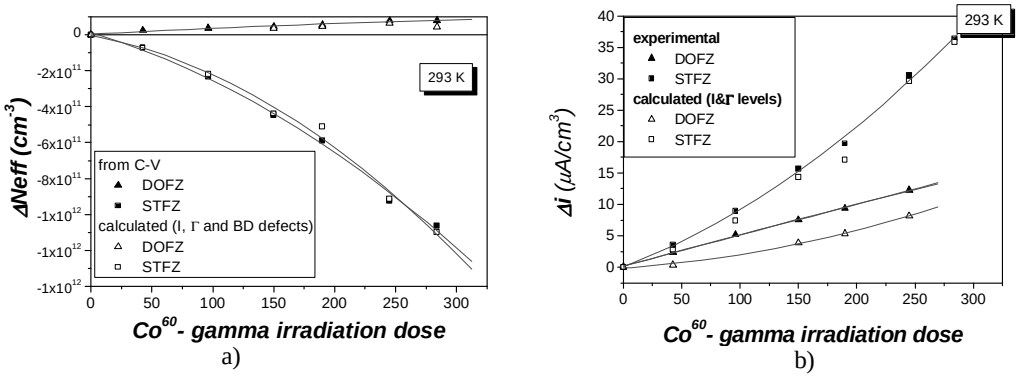

Fig. 19. Experimental results and calculations for the change of the space charge density (a) and the leakage current (b) [38].

8. A super-radiation-hard silicon detector for future high energy physics experiments

While the RD48 approach for defect engineering of silicon detectors (DOFZ technology) had proven to be sufficient to guarantee their operability throughout the LHC experiments, the much higher demand for the LHC upgrade (SLHC) could not be fulfilled. Possible solutions are now the prime focus of the CERN-RD50 collaboration. One possible approach was studied recently within the Hamburg group and will be briefly outlined here [42]. As to the design implications as given by SLHC experiments small area thin pixel detectors are the logical choice for the innermost layers of the tracking detector. This implies the possibility of using material with much higher doping concentration, for which an appreciably lower donor removal constant could be expected thus shifting the type inversion to equivalently higher fluence values. On top of this it was found that the donor creation as first shown in the gamma irradiated DOFZ diodes (Fig. 16, 17 and 19(a)) plays an important role too, although the technology used here (epi-layers, ρ = 50 Ωcm, d = 50 μm) does not use any intentional oxygen enrichment. Experiments have shown that these devices are highly superior to any standard or oxygenated float zone silicon devices and that contrary to those the epi diodes do not exhibit any type inversion effect (see Fig. 20). The effect is attributed to damage induced generation of the bistable donor BD, tentatively assigned as thermal double donor TDD (see section 7). A distinct difference between the TSC spectra, displayed in Fig. 21, [43] for FZ and epi diodes is observed. The epi sample shows in contrast to the FZ one a complete absence of the I-level and in the 80-100 K range the already mentioned BD (identification as shallow donor via the Pool-Frenkel effect), whereas in L(90) seen for the FZ sample much of the intensity for the donor state of the I-level is contained [40].

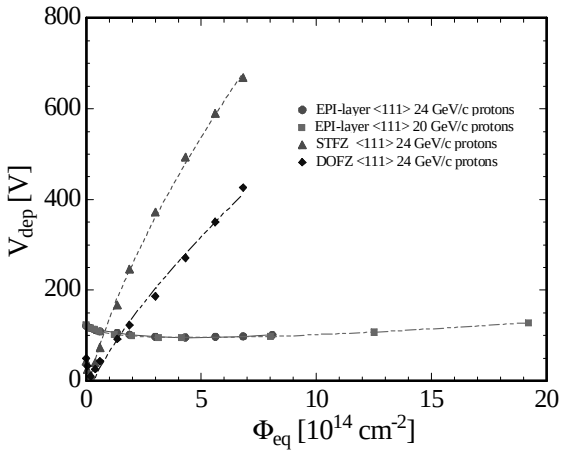

Fig. 20. CERN-scenario experiment (as in Fig. 11) comparing the depletion voltage needed for FZ and epi diodes as function of fluence [42] (update).

A tentative explanation for the donor generation in epi diodes is based on the fact that oxygen dimers present in the Cz-substrate will predominantly migrate into the epi-bulk during the growth process, such that the ratio of dimers to interstitial Oxygen is much higher in epi than in standard or even oxygenated FZ silicon. Dimers are known to be precursors for irradiation induced thermal donor generation thus leading to an increase of the net positive space charge, more than balancing the negative space charge generation seen in FZ devices due to generation of deep acceptors.

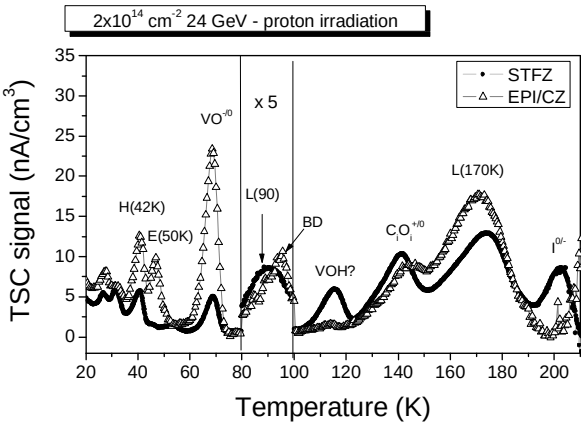

Fig. 21. TSC spectrum measured after proton irradiation; comparison btween FZ and epi diodes [43].

Finally a preliminary analysis of the annealing functions for N_{eff} had been undertaken and used for an operational projection in the SLHC environment. The results are very promising and show that according to a proper temperature scenario for the off beam periods the adverse effect of acceptor generation due to reverse annealing can always be balanced by the donor generation such that the operational voltage would not change during the entire SLHC experimental period. In addition trapping effects (charge collection efficiency CCE) had been measured. Although the trapping time constants are the same as measured for FZ-diodes, the thickness of only 50 μm has led to a CCE value of 50%, obtained after $\Phi_{eq} = 1 \times 10^{16}$ cm^{-2}, which is regarded to be sufficient for SLHC operation.

9. Conclusions

It has been shown that starting from a rather pragmatic approach of try and error the involvement of proper semiconductor analysis tools leads to a first understanding of the complex damage effects in high resistivity silicon particle detectors and may finally be used for intentional defect engineering design of detectors with superior radiation tolerance being capable to withstand the unprecedented challenge imposed on such detectors by the next generation of high energy physics experiments. The first results obtained with thin low resistivity epi diodes, presented in section 8, are extremely promising in this respect. Systematic work on this subject will be continued within the frame of the CERN RD50 collaboration, for forthcoming updates see [23].

References

[1] K. McKay, Phys. Rev. **76**, 1537 (1949).
[2] J. Kemmer, Nucl. Instr. Meth. A **169**, 499 (1980).
[3] G. Lutz, Semiconductor Radiation Detectors, Springer-Verlag 1999.
[4] A. Holmes-Siedle, Len Adams, Handbook of Radiation Effects, 2nd Edt., Oxford University Press, 2002.
[5] 7th International Conference on Advanced Technology and Particle Physics, Villa Olmo, Como, Italy, Oct. 2001, Proceedings on ICATPP-7, Editors M. Barone, E. Borchi, J. Huston, C. Leroy, P. G. Rancoita, P. Riboni, R. Ruchti, World Scientific Publishing, Singapore 2003.
[6] New Developments in Radiation Detectors, Proceedings of the 9th European Symposium on Semiconductor Detectors, Schloss Elmau, Bavaria, Germany, June 23-27, 2002, Editors P. Holl, G. Lutz, F. Schopper, L. Strüder, S. Masciocchi, C. Fiorini, A. Longo, M. Sampietro, Nucl. Instr. and Meth. A 512, Nos. 1-2 (2003).
[7] Proceedings of the 4th Intern Conf. on Radiation Effects on Semiconductor Materials, Detectors and Devices, Florence, Italy, July 10-12, 2002, Editors E. Borchi, M. Bruzzi, Nucl. Instr. and Meth. A 514, Nos. 1-3 (2003).

[8] Proceedings of the International Workshop on Semiconductor Pixel Detectors for Particles and X-Rays (PIXEL 2002), Carmel, California, USA, Sept.9-12, 2002, Editor S.C. Loken, eConf C020909.
[9] Nuclear Science (NSS/MIC) 2002 IEEE Symposium and Medical Imaging, Conference, Nov. 2002, Norfolk, Virginia, USA, Conference.
[10] Proceedings of the 11th International Workshop on Vertex Detectors, VERTEX 2002, Hawaii, USA, November 3-8, 2002, Editors S.L. Olsen, D. Bortoletto, Nucl. Instr. and Meth. A, Nos. 1-2 (2003).
[11] Frontier Detectors for Frontier Physics, 9th Pisa meeting on advanced detectors, La Biodola, Elba, Italy, May 25-31, 2003, to be published. in Nucl. Instr. and Meth. A.
[12] LHC, The Large Hadron Collider Home Page: http://lhc-new-homepage.web.cern.ch/lhc-new-homepage/.
[13] TESLA, The Tera Electron Volt Energy Superconducting Linear Accelerator Home Page: http://tesla.desy.de/.
[14] ATLAS, A Toroidal LHC ApparatuS, http://atlas.web.cern.ch/Atlas/Welcome.html
[15] T. Rohe, Paul Scherrer Institut PSI Villigen, Switzerland, Seminar talk at Hamburg University, June 2003.
[16] CMS, The Compact Muon Solenoid, http://cmsinfo.cern.ch/Welcome.html/.
[17] F. Gianotti, M. L. Mangano, T. Virdee, S. Abdullin, G. Azuelos, A. Ball et al.., Physics potential and experimental challenger of the LHC luminosity upgrade, CERN-TH/2002-078, hep-ph/0204087F. Gianotti et al., Physics potential and experimental challenger of the LHC luminosity upgrade, CERN-TH/2002-078, hep-ph/0204087.
[18] M. Huhtinen, Nucl. Instr. and Meth. A **491**, 194 (2002),
[19] G. Lindström, Radiation Damage in Silicon Detectors, Nucl. Instr. and Meth. A **512**, 30 (2003).
[20] RD48 Status report, CERN/LHCC 2000-009, December 1999.
[21] Rose collaboration: http://rd48.web.cern.ch/RD48.
[22] G. Lindström et al.(RD48), Nucl. Instr. and Meth. A 466 (2001) 308.
[23] RD50 collaboration, http://rd50.web.cern.ch/rd50/.
[24] Z. Li, Ultra-rad-hard Sensors for Particle Physics Applications, in [8]: http://www.slac.stanford/edu/econf/C020909/zlpaper.pdf.
[25] M. Moll, Nucl. Instr. And Meth. A **511**, 97 (2003).
[26] M. Bruzzi, Development of radiation hard semiconductor detectors for very high luminosity colliders, in [11].
[27] R. Wunstorf, Nucl. Instr. And Meth. A **466**, 327 (2001).
[28] M. Moll, Ph.D. thesis, Hamburg University 1999, DESY-THESIS-1999-040, ISSN-1435-8085.
[29] R. Wunstorf, Ph.D. thesis, Hamburg University 1992, DESY FH1K-92-01 (October 1992).
[30] G. Kramberger, Ph.D. thesis, University of Ljubljana 2001, and IEEE Trans. Nucl. Sci. **49**(4), 1717 (2002).
[31] A. Ruzin (RD48), Nucl. Instr. and Meth. A **447**, 116 (2000).
[32] M. Moll, E. Fretwurst, M. Kuhnke, G. Lindström, Nucl. Instr. and Meth. in Phys. Res. B **186**, 100 (2002).
[33] B. C. MacEvoy, Nucl. Instr. and Meth. A **388**, 365 (1997).
[34] S. Lazanu, I. Lazanu, J. Optoelectron. Adv. Mater. **5**(3), 647 (2003).
[35] Z. Li, B. Dezillie, M. Bruzzi, W. Chen, V. Eremin, E. Verbitskaya, P. Weilhammer, Nucl. Instr. and Meth. A 461, 126 (2001).
[36] I. Pintilie, E. Fretwurst, G. Lindström, J. Stahl, Appl. Phys. Letters **81**(1) 165 (2002).
[37] I. Pintilie, E. Fretwurst, G. Lindström, J. Stahl, Appl. Phys. Letters **82**(13), 2169 (2003).
[38] I. Pintilie, E. Fretwurst, G. Lindström, J. Stahl, Nucl. Instr. and Meth. A **514**, 18 (2003).
[39] E. Fretwurst, G. Lindström, J. Stahl, I. Pintilie, Z. Li, J. Kierstead, E. Verbitskaya, R. Röder, Nucl. Instr. and Meth. A **514**, 1 (2003).
[40] I. Pintilie, E. Fretwurst, G. Kramberger, G. Lindstroem, Z. Li, J. Stahl, Physica B **340-342**, 578 (2003).
[41] H. Lee, J. Corbett, Phys. Rev. B **13**(6), 2563 (1976).
[42] G. Kramberger, D. Contarato, E. Fretwurst, F. Hönniger, G. Lindström, I. Pintilie, R. Röder, A. Schramm, J. Stahl, Nucl. Instr. and Meth. A **515**, 665 (2003).
[43] J. Stahl, E. Fretwurst, G. Lindstroem, I. Pintilie, Physica B **340-342**, 705 (2003).